

Article

Comparative Transcriptomic Profiling of Brain and Liver in Phoenix Barbs (*Spinibarbus denticulatus denticulatus*) with Differential Growth Rates

Xi Xie ¹ , Jiamiao Zhuang ¹, Xianping Liao ², Zhengsheng Xu ², Wenlang Liang ², Yilin Su ², Li Lin ³, Jungang Xie ^{2,*} and Weiqiang Lin ^{2,*}

¹ Guangdong Provincial Key Laboratory of Lingnan Specialty Food Science and Technology, College of Light Industry and Food, Zhongkai University of Agriculture and Engineering, Guangzhou 510225, China; xixie31@hotmail.com (X.X.); zhuangjiamiao@hotmail.com (J.Z.)

² Fishery Research Institute of Zhaoqing, Zhaoqing 526114, China; xianpingliao1993@hotmail.com (X.L.); xuzs331@outlook.com (Z.X.); lw1012104@hotmail.com (W.L.); yilinsu@sina.com (Y.S.)

³ Guangdong Provincial Water Environment and Aquatic Products Security Engineering Technology Research Center, Guangzhou Key Laboratory of Aquatic Animal Diseases and Waterfowl Breeding, College of Animal Science Technology, Zhongkai University of Agriculture and Engineering, Guangzhou 510225, China; linli@zhku.edu.cn

* Correspondence: xjg1113@outlook.com (J.X.); lwq20240905@hotmail.com (W.L.); Tel.: +86-07582230344 (J.X.); +86-07582612032 (W.L.)

Abstract: Phoenix barb (*Spinibarbus denticulatus denticulatus*) is a notable fish species in South China and is valued for its ecological and economic importance. To elucidate the molecular basis underlying its growth, we collected transcriptome profiles from the brains and livers of individual fish with different growth rates and compared differentially expressed genes (DEGs) at 3 and 9 months after hatching (MAH). Kyoto Encyclopedia of Genes and Genomes (KEGG) analysis revealed that the pathways associated with growth were predominantly enriched in fatty acid biosynthesis, AMPK signaling, PI3K-Akt signaling, estrogen signaling, and protein metabolism. Notably, a greater number of DEGs from the fast-growing group were associated with these pathways at the early growth stage (3 MAH) than at the later stage (9 MAH). Real-time quantitative PCR results further validated that the genes involved in these pathways exhibited higher expression levels in fast-growing samples. This study enhances our understanding of the genetic mechanisms underlying growth rate differences and provides valuable genetic resources for future growth-related molecular breeding programs of phoenix barbs.

Keywords: brain and liver; *Spinibarbus denticulatus denticulatus*; growth and development; transcriptome analysis

Key Contribution: The study investigates the brains and liver transcriptomes between fast- and slow-growing phoenix barbs and reveals the differentially expressed genes from these two tissues at two stages, offering insights for potential selective breeding strategies in this species.



Citation: Xie, X.; Zhuang, J.; Liao, X.; Xu, Z.; Liang, W.; Su, Y.; Lin, L.; Xie, J.; Lin, W. Comparative Transcriptomic Profiling of Brain and Liver in Phoenix Barbs (*Spinibarbus denticulatus denticulatus*) with Differential Growth Rates. *Fishes* **2024**, *9*, 411. <https://doi.org/10.3390/fishes9100411>

Academic Editor: Giacomo Zaccane

Received: 3 September 2024

Revised: 4 October 2024

Accepted: 10 October 2024

Published: 13 October 2024



Copyright: © 2024 by the authors. Licensee MDPI, Basel, Switzerland. This article is an open access article distributed under the terms and conditions of the Creative Commons Attribution (CC BY) license (<https://creativecommons.org/licenses/by/4.0/>).

1. Introduction

Fish growth rate is the increase rate of body weight, body length, and body height and is an economic trait for fish production. The growth rate of farmed fish directly influences production efficiency. A higher growth rate leads to faster turnover in fish production, resulting in greater economic benefits from aquaculture. Based on previous studies, environmental stress, disease, energy metabolism, and genetic heritability values can influence the growth status of fish [1–4]. In recent decades, many artificial selection practices have shown that desirable growth traits can be obtained by phenotyping fish species and that

many individual fish with outstanding traits can be used for artificial breeding [5]. However, identifying individuals with stable, promising phenotypes is challenging because environmental factors and genetic bases determine most phenotypes, and heritable phenotypes mainly originate from their genetic background [5,6]. Therefore, understanding the genetic characteristics of superior individuals is becoming increasingly important in fish breeding [5]. With the development of genetics and sequencing technologies of fish, more and more gene-related biomarkers have been selected and used for breeding selection in aquaculture, with the advantages of low labor cost, rapid detection, and stable selection [7,8]. However, the process is complicated and poorly understood [9,10].

To acquire more genetic information on economically important traits, identifying molecular mechanisms and regulatory pathways is essential for understanding key genes involved in fish growth. Numerous studies indicated that the growth of fish is primarily regulated by the brain–liver axis [11–13]. The brain plays a key role in growth regulation by secreting hormones involved in growth and reproduction control [14–17]. The liver is responsible for metabolizing and storing essential nutrients, such as carbohydrates, fats, and proteins. In the brain–liver axis, the liver influences the central nervous system by regulating feeding behavior, while signals from the brain affect glucose, lipid, and protein metabolism in the liver [18]. For example, growth hormone (GH), gonadotropin hormone-releasing hormone (GnRH), and growth hormone-releasing hormone (GHRH) are the major genes in the brain–liver axis that encode hormones secreted by the hypothalamus [11–13] and insulin-like growth factors (IGFs) released from liver. Furthermore, the growth factors (GFs) gradually stimulate the liver and other target organs [3,19,20]. For example, Mun et al. discovered that juvenile red spotted groupers (*Epinephelus akaara*) with varying growth rates exhibited distinct levels of hormone pathway genes in the brain, liver, and muscle tissues [21]. They found that the hormone status and growth rate of different species could be altered by controlling the concentrations of growth hormones. Xue et al. indicated that the gene IGF1 from the growth hormone (GH)/insulin-like growth factor system is upregulated in fast-growing grass carp (*Ctenopharyngodon idella*) [1]. However, IGF1 is highly expressed in hepatic and non-hepatic tissues in several fish species [22–24]. Therefore, identifying genes involved in the brain–liver axis and understanding the cross-linkage of the related pathways can reveal the molecular genetic mechanisms on fish growth and provide a theoretical foundation for growth promotion.

Recently, transcriptome sequencing has been extensively used to investigate gene expression across various growth stages and environmental conditions. Yang et al. conducted transcriptome sequencing of the brain, liver, and muscle tissues of 3-month-old zig-zag eels (*Mastacembelus armatus*) with varying growth rates. Multiple growth-related genes and biological pathways were identified, revealing that GH and growth hormone receptors (GHRs) play crucial roles in early development. Lin et al. used transcriptome sequencing technology to conduct QTL mapping and identify significant candidate genes associated with tilapia growth and omega-3 fatty acid content [25]. Subsequently, traits from the candidate genes were selected for breeding based on the identified SNPs. Numerous studies have utilized transcriptomes to elucidate the genes associated with individual differences in growth rates, particularly those related to pathways such as fatty acids, amino acids, and signaling [26–28]. For example, Charles et al. found the IGF1 and IGF3 are associated with golden pompano growth, and that muscle development responds to the mRNA expression levels of these two genes in a dose- and time-dependent manner [29]. In addition, GHs may represent a direct indicator of the effects of acute and chronic stressors on *Pampus argenteus* growth [30]. These findings provide valuable insights into the genetic basis of variation in growth rates. Identification of these genes can help people understand the growth mechanisms of organisms, and bio-markers for selective breeding offer specific target genes for further study.

The Chinese phoenix barb (*Spinibarbus denticulatus denticulatus*) belongs to the family Cypriniformes and is primarily found in upper rivers [31,32]. This species is well-known for its tender flesh and exquisite taste, which makes it economically valuable for production.

However, the growth rate of this species is slower than that of other fish. To develop fish families with fast-growth traits, selecting individuals with fast growth rates is essential for the breeding and conservation of *S. d. denticulatus*. Additionally, our knowledge of the molecular mechanism of brain–liver axis regulation of *S. d. denticulatus* growth remains limited. Therefore, identifying the key genes associated with the growth of *S. d. denticulatus* and discovering potential genetic markers for the selection of individuals with fast-growth traits are beneficial to *S. d. denticulatus* breeding. In this study, a correlation analysis of the transcriptome from the whole brain and liver of *S. d. denticulatus* was conducted. Thus, the molecular mechanisms underlying the growth of the *S. d. denticulatus* were further clarified.

2. Materials and Methods

2.1. Collection of Animal Samples

S. d. denticulatus were purchased from Zhaoqing Fisheries Research Institute. The original parental phoenix barbs were collected from the Xijiang River, and the first generations were obtained by mating a sire and a dam. The next generation of fish was cultivated under standardized feeding management conditions, and 80 individuals with both fast and slow growth rates were screened and labeled with barcodes. During the experiment, the fish were fed twice daily (at 9:00 A.M. and 5:00 P.M.) at a daily feeding rate of 3.0% of their body weight. This rate was adjusted based on water temperature (18–25 °C) and feeding behavior to ensure uniform feeding. Mortality, feed intake, and other observations were recorded daily throughout the duration of the rearing period.

For each group, 20 individuals were selected and divided into four samples, with five individuals combined to form each sample. Fish that were selected were anesthetized as soon as possible in a 10 L plastic bucket with 20 mg/L clove oil [33]. Growth parameters (weight, body length, and width) were measured at 3 and 9 months after hatching (MAH). Brain and liver tissues were collected for transcriptome sequencing. All collected tissue samples were stored in clean sample tubes, flash-frozen with liquid nitrogen, and immediately transferred to −80 °C.

2.2. RNA Extraction Sample

Total RNA was extracted from the brain and liver tissues using TRIzol kits (TaKaRa, Dalian, China). After treatment with DNase I (TaKaRa, Dalian, China) to remove genomic DNA interference, the RNA content was analyzed by 1% agarose gel electrophoresis. RNA purity and quantity were determined using an ultra-microvolume spectrophotometer (Thermo Scientific, Shanghai, China). Four replicate pools of mixed RNA samples from fish with varying growth rates and eight replicate pools of samples from fish with the two growth stages were collected. These were used to construct cDNA libraries to facilitate differential expression analysis. Total RNA samples underwent mRNA enrichment, followed by mRNA fragmentation using a fragmentation buffer. Subsequently, the second strand was synthesized using random N6 primers for reverse transcription into cDNA, forming double-stranded DNA. The double-stranded DNA fragments were blunt-ended and phosphorylated for forming a sticky overhang with an “A”. The ligated products were amplified by random primers. The PCR product was denatured to a single strand for developing a DNA library. The library was then sequenced using a sequencing machine.

2.3. Library Generation and RNA-seq Analysis

The cDNA library was sequenced using a HiSeq 2000 sequencing platform (BGI Genomics Shenzhen Co., Ltd., Shenzhen, China). The reads were filtered using SOAPnuke, software developed independently by BGI, to remove junk reads. After consolidating the assembly results from multiple samples, clean reads were aligned to the genome sequence using Bowtie2 [34]. Subsequently, gene expression levels in each sample were calculated using RSEM. Differential gene analysis within groups was conducted using DESeq, with a fold change ≥ 2 and an adjusted p -value ≤ 0.001 . The DEGs were functionally categorized by Gene Ontology (GO) and Kyoto Encyclopedia of Genes and Genomes (KEGG). KEGG

enrichment analysis was conducted using R software, while GO enrichment analysis was performed using the TermFinder package with a Q-value ≤ 0.05 as the threshold; meeting this condition is defined as a significant enrichment in candidate genes. The number of differentially expressed genes in the slow-growing (SG) group at the three growth stages compared with the fast-growing (FG) group was determined using the edgeR package [6]. All individual genes were annotated using NCBI non-redundant (NR) proteins, Eukaryotic Homologous Taxa (KOG), KEGG, NCBI Nucleotides (NT), and Gene Ontology (GO). The transcriptome sequencing data used in this study were deposited in the NCBI Short Read Archive (SRA).

2.4. Reverse Transcription Quantitative PCR Analysis

The expression profiles of six selected DEGs determined by real-time quantitative reverse transcription PCR (qRT-PCR) to validate the transcriptome data. The primers for qRT-PCR were designed using Primer Premier 5.0 and listed in Supporting Information Table S1. RT-qPCR was performed using SYBR Green Master Mix (Vazyme Biotech Co., Nanjing, China). The PCR conditions were as follows: 50 °C for 2 min, 95 °C for 2 min, 40 cycles of 95 °C for 5 s, 60 °C for 1 min and 1 cycle of 95 °C for 15 s, 60 °C for 1 min and 95 °C for 15 s for melting curve analysis. The β -actin gene was used as the control, and the expression of the genes was corrected to that of the control using the $2^{-\Delta\Delta C_t}$ method [35,36].

2.5. Statistical Analysis

All statistical analyses were performed using Sigmaplot 12.5 (Sigmaplot, San Francisco, CA, USA). Significant differences between experimental groups were analyzed using ANOVA, and all data are presented as mean \pm standard deviation (S.D.). Statistical significance was set at $p < 0.05$.

2.6. Ethical Statement

The care and use of experimental animals complied with Zhongkai University of Agriculture and Engineering animal welfare laws, guidelines, and policies as approved by the Care and Use of Laboratory Animals Committee of Zhongkai University of Agriculture and Engineering (no. 2020071109).

3. Results

3.1. Growth Performance of FG and SG *S. d. denticulatus*

Phenotypic indices (weight, body length, body width, body height, and head width) were measured at different growth stages in the FG and SG groups. No significant differences were observed in weight, body length, or height between the two groups at 3 MAH, but significant differences in these parameters were observed at 9 MAH. There were 2.3-, 1.4-, 1.3-, 1.33-, and 1.4-fold increases in body weight, length, thickness, height, and head length of FG individuals, respectively, compared to the SG group at 9 MAH (Table 1). Although the table did not show the statically significant differences between the FG and SG groups at 3 MAH, the data clearly showed that the FG group had heavier body weights and longer body lengths relative to SG group.

Table 1. Growth parameters of Chinese phoenix barb (*S. d. denticulatus*) in the FG and SG groups at different sampling times.

	3 MAH		9 MAH	
	FG	SG	FG	SG
Body Weight (g)	13.88 \pm 0.65 ^c	11.63 \pm 0.36 ^d	74.80 \pm 2.04 ^a	32.23 \pm 1.45 ^b
Body Length (cm)	86.45 \pm 1.44 ^c	83.40 \pm 1.17 ^d	166.00 \pm 1.63 ^a	120.60 \pm 3.55 ^b
Body Width (cm)	13.55 \pm 0.30 ^c	12.18 \pm 1.06 ^c	23.95 \pm 0.29 ^a	17.40 \pm 0.43 ^b
Body Height (cm)	25.60 \pm 0.56 ^c	23.10 \pm 1.73 ^c	46.85 \pm 0.63 ^a	32.10 \pm 0.99 ^b
Head Length (cm)	20.70 \pm 0.33 ^c	19.80 \pm 0.63 ^c	33.95 \pm 0.28 ^a	27.30 \pm 0.87 ^b

Note: Means with the same letter are not significantly different. (Statistical analysis was conducted using one-way analysis of variance ($p < 0.05$)).

3.2. Sequencing and Annotation

Comparative analysis of brain and liver tissues from FG and SG *S. d. denticulatus* was performed. The analysis showed an average of 42,710,766; 42,734,416; 42,602,648; 42,046,944; 42,374,386; 42,633,500; 42,283,976; and 42,213,928 clean reads for 3MAH-FG-LIVER, 3MAH-SG-LIVER, 3MAH-FG-BRAIN, 3MAH-SG-BRAIN, 9MAH-FG-LIVER, 9MAH-SG-LIVER, 9MAH-FG-BRAIN, and 9MAH-SG-BRAIN, respectively, with a total of 81.03 Gb of clean bases. The GC content ranged from 46.34% to 48.37% of the sequencing data, with Q20 > 96%, which was used for subsequent analysis (Table S2). All the SRA data were submitted to the NCBI for the Biotechnology Information Sequence Read Archive database (PRJNA848289).

3.3. Identification of DEGs in Liver and Brain Tissues at Two Developmental Stages

The number of DEGs that were up- and downregulated between the FG and SG groups was assessed at 3 and 9 MAHs in the brain and liver tissues. In the brain, 570 upregulated DEGs and 532 downregulated DEGs were observed at 3 MAH, whereas 856 upregulated DEGs and 540 downregulated DEGs were observed at 9 MAH (Figure 1a). In the liver, 417 upregulated and 389 downregulated DEGs were observed at 3 MAH. Notably, a substantial increase in DEGs was observed at the later stage, with 2086 upregulated and 1081 downregulated DEGs at 9 MAH (Figure 1b).

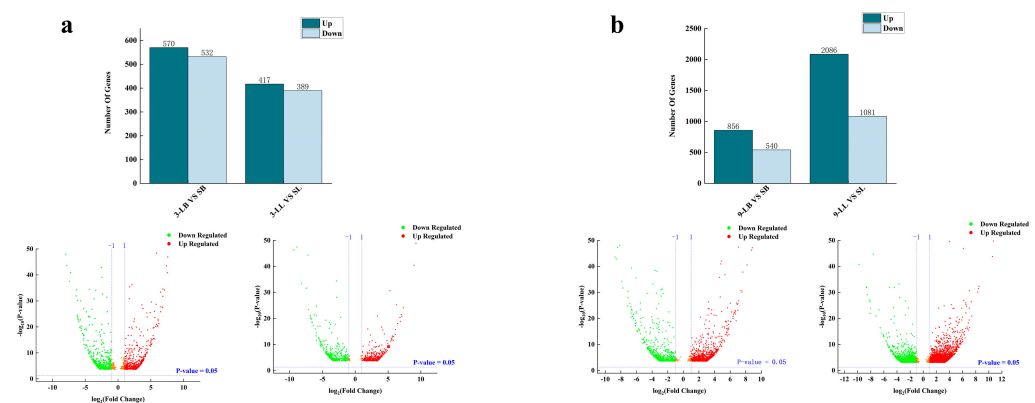


Figure 1. Analysis of DEGs in the brain and liver tissues of *S. d. denticulatus* in the FG and SG groups. (a) numbers of up- or down-regulated genes from brain and liver tissue at 3 MAH. (b) numbers of up- or down-regulated genes from brain and liver tissue at 9 MAH. FB, brain sample from the FG group; SB, brain sample from the SG group; FL, liver sample from the FG group; SL, liver sample from the SG group.

3.4. Analysis of DEGs between FG and SG *S. d. denticulatus*

GO analysis of DEGs in *S. d. denticulatus* brain tissue revealed that DEGs in the FG and SG groups were enriched in 24 GO terms at 3 MAH (Figure 2a). Among these, the four significantly enriched terms were alpha-amino acid metabolic process (GO:1901605), protein metabolic process (GO:0019538), regulation of signal transduction (GO:0009966), and response to stimulus (GO:0050896). At 9 MAH (Figure 2b), the DEGs in the FG and SG groups were located in 32 GO terms, with the top enriched terms being cellular component assembly (GO:0022607), cell adhesion (GO:0007155), and transport (GO:0006810). GO analysis of the DEGs in the liver tissues of *S. d. denticulatus* revealed that the DEGs in the FG and SG groups were enriched in 30 GO terms at 3 MAH (Figure 2c). Among these, the following three terms were significantly enriched: alpha-amino acid metabolic process (GO:1901605), neuron projection development (GO:0042446), and neuron projection organization (GO:0031175). Moreover, at 9 MAH (Figure 2d) DEGs in both groups were enriched with 33 GO terms. The three most enriched terms at this time point were hormone biosynthetic process (GO:0022607), regulation of cellular metabolic process (GO:0031323), and response to other organisms (GO:0051707).

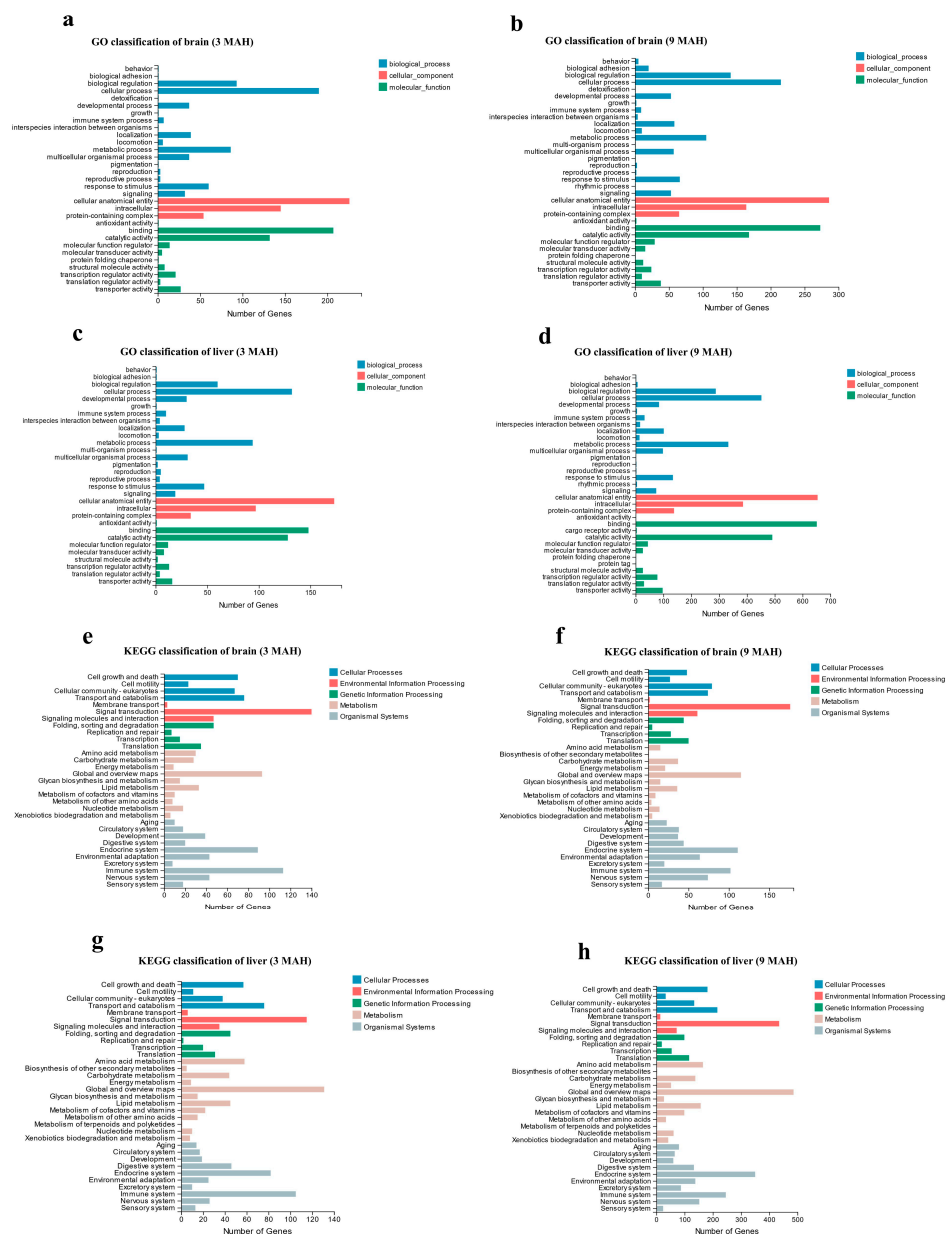


Figure 2. GO and KEGG analyses of DEGs in the brain and liver tissues of the FG and SG groups of *S. denticulatus*. (a) Brain tissue differential expression genes GO classification at 3 MAH; (b) brain tissue differential expression genes GO classification at 9 MAH; (c) liver tissue differential expression genes GO classification at 3 MAH; (d) liver tissue differential expression genes GO classification at 9 MAH; (e) Brain tissue differential expression genes KEGG classification at 3 MAH; (f) brain tissue differential expression genes KEGG classification at 9 MAH; (g) liver tissue differential expression genes KEGG classification at 3 MAH; (h) liver tissue differential expression genes KEGG classification at 9 MAH.

The annotation results of the DEGs in the brain tissue at 3 and 9 MAH were classified according to the pathway categories in the KEGG database. We found that 31 KEGG pathways were enriched in the FG and SG groups at 3 MAH, whereas 32 pathways were enriched at 9 MAH (Figure 2e–h). Among them, the main enriched term was the signal transduction pathway for the environmental information process category for both 3 and 9 MAH, whereas the enriched term for metabolism was lipid metabolism. In terms of cellular processes, transport and catabolism pathways were enriched at 3 MAH, whereas the cell community–eukaryote pathway was enriched at 9 MAH. For genetic information

processing, the folding, sorting, and degradation pathways showed the highest gene expression at 3 MAH, whereas the translation pathway showed the highest level of gene expression at 9 MAH. In the organism system, the endocrine and immune system pathways were enriched at 3 MAH, whereas the endocrine system pathway was enriched at 9 MAH. In the liver tissue, DEGs in the FG and SG were enriched in 34 and 33 KEGG pathways at 3 and 9 MAH, respectively. The main enrichment at 9 MAH was in the transport and catabolic metabolic pathways. Therefore, the enriched pathways in liver tissue were consistent with those in brain tissue.

3.5. Analysis of DEGs between the FG and SG Groups at Two Growth Stages

To elucidate the expression patterns at different growth stages in the brain and liver tissues, DEGs at the two growth stages in either brain or liver samples were compared. KEGG analysis showed that these DEGs were mainly enriched in the IL-17 signaling pathway; Th17 cell differentiation; the estrogen signaling pathway; the NOD-like receptor signaling pathway; valine, leucine, and isoleucine degradation; fatty acid elongation; propanoate metabolism; and the PI3K-Akt signaling pathway at 3 MAH (Figure 3a). At 9 MAH, DEGs were mainly enriched in O-glycan biosynthesis, insulin secretion, the thyroid hormone signaling pathway, the GnRH signaling pathway, and the sphingolipid signaling pathway in the brain (Figure 3b). In liver tissues, the DEGs at 3 MAH showed enrichment in amino acid metabolism, lipid metabolism, fat digestion and absorption, the GHRH pathway, and the IL-17 signaling pathway (Figure 3c). The DEGs at 9 MAH were observed in glycerolipid metabolism; the FoxO signaling pathway; the PPAR signaling pathway; glycine, serine, and threonine metabolism; the AMPK signaling pathway; and the insulin signaling pathway (Figure 3d).

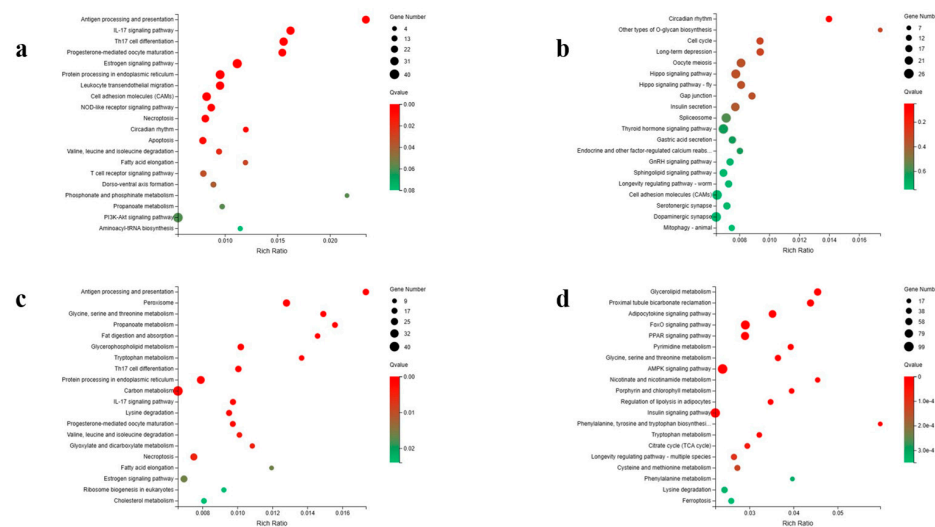


Figure 3. Enrichment analysis of common differentially expressed genes in KEGG pathways in the brain and liver tissues of *S. d. denticulatus* from the FG and SG groups at two growth stages. The following maps show the concentration of differentially expressed genes in brain tissue: (a) Brain tissue KEGG concentration map at 3 MAH, (b) brain tissue KEGG concentration map at 9 MAH, (c) liver tissue KEGG enrichment map at 3 MAH, (d) liver tissue KEGG enrichment map at 9 MAH.

3.6. Analysis of DEGs from the Brain–Liver Axis

As shown in Figure 4, there were 199 and 276 common DEGs at 3 and 9 MAH from the two tissues, respectively. To assess the relationship between growth performance and gene expression within the brain–liver axis, genes and enriched pathways were identified in the these tissues. Comparison of the DEGs from the two tissues indicated that the DEGs from lipid elongation, the PI3K-Akt signaling pathway, the GHRH pathway, and the IL-17 signaling pathway were enriched at 3 MAH, whereas the insulin signaling pathway co-existed in both tissues at 9 MAH. For example, in the early growth stage, two downregulated and

two upregulated DEGs were identified in the lipid elongation pathway, six downregulated and two upregulated genes were detected in the Th17 cell differentiation pathway, and three downregulated and two upregulated genes were enriched in the IL-17 signaling pathway. Similarly, at the later stage, the insulin signaling pathway showed 10 downregulated and 2 upregulated genes in the two tissues (Table 2). Heatmap analysis showed selected common DEGs in brain and liver tissues. Most of these common DEGs showed similar trends in the brain and liver (Figure 5). For example, enoyl-CoA hydratase was upregulated in the early growth stage in both the brain and liver, whereas it was downregulated at a later stage in these two tissues.

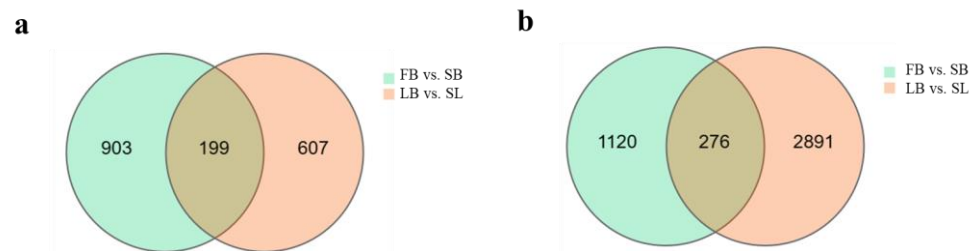


Figure 4. Global overview of DEGs based on Venn diagram analysis. (a) Venn diagram of DEGs from brain and liver tissues at 3 MAH. (b) Venn diagram of DEGs from brain and liver tissues at 3 and 9 MAH. FB, brain sample from the FG group; SB, brain sample from the SG group; FL, liver sample from the FG group; SL, liver sample from the SG group.

Table 2. Differential expression of 3 and 9 MAH genes in the brain tissue of *S. d. denticulatus* in the FG and SG groups.

Tissue	Period	Gene ID	Gene Description	Fold Change	p Value
Brain	3 MAH		Th17 cell differentiation		
		isoform_86026	molecular chaperone HtpG	8.34	<0.01
		isoform_378722	proto-oncogene protein c-fos	3.26	<0.01
		isoform_32558	splicing factor, arginine/serine-rich 1	2.14	<0.01
		isoform_132081	solute carrier family 30 (zinc transporter), member 10	1.35	<0.01
			IL-17 signaling pathway		
		isoform_354536	hypoxia-inducible factor 1 alpha	3.35	<0.01
			Estrogen signaling pathway		
		isoform_222321	GTPase KRas/Thermogenesis	2.85	<0.01
		isoform_242870	calmodulin	2.78	<0.01
		isoform_268095	heat shock 70 kDa protein 1/2/6/8	2.29	<0.01
			NOD-like receptor signaling pathway		
		isoform_270527	mitochondrial FAD-linked sulphydryl oxidase	2.79	<0.01
		isoform_132081	solute carrier family 30 (zinc transporter), member 10	1.35	<0.01
		isoform_221836	ryanodine receptor 3	1.19	<0.01
			Valine, leucine, and isoleucine degradation		
		isoform_296751	methylmalonyl-CoA mutase	6.33	<0.01
		isoform_38010	acetyl-CoA acyltransferase 2	2.82	<0.01
		isoform_228961	dihydrolipoamide dehydrogenase	2.67	<0.01
			Fatty acid elongation		
		isoform_331832	long-chain 3-hydroxyacyl-CoA dehydrogenase	3.84	<0.01
		isoform_38010	acetyl-CoA acyltransferase 2	2.82	<0.01
		isoform_213152	very-long-chain (3R)-3-hydroxyacyl-CoA dehydratase	2.80	<0.01
			Propanoate metabolism		
		isoform_296751	methylmalonyl-CoA mutase	6.33	<0.01
		isoform_331832	enoyl-CoA hydratase	3.84	<0.01
		isoform_360405	L-lactate dehydrogenase	3.25	<0.01
		isoform_228961	dihydrolipoamide dehydrogenase	2.67	<0.01
			PI3K-Akt signaling pathway		
		isoform_73678	14-3-3 protein gamma/eta	2.92	<0.01
		isoform_222321	GTPase KRas	2.85	<0.01
		isoform_232012	thrombospondin 1	2.52	<0.01
		isoform_342907	cytochrome c oxidase assembly protein subunit 11	2.16	<0.01
		isoform_263042	GTPase HRas	2.12	<0.01

Table 2. Cont.

Tissue	Period	Gene ID	Gene Description	Fold Change	p Value
Brain	9 MAH		O-glycan biosynthesis		
		isoform_368717	beta-galactoside alpha-2,6-sialyltransferase	4.53	<0.01
		isoform_168720	protein O-GlcNAc transferase	2.73	<0.01
			Insulin secretion		
		isoform_32522	guanine nucleotide-binding protein subunit alpha-11	4.92	<0.01
		isoform_166285	pituitary adenylate cyclase-activating polypeptide type I receptor	3.12	<0.01
		isoform_179654	SWI/SNF-related matrix-associated actin-dependent regulator of	3.03	<0.01
			chromatin subfamily A member 2/4		
		isoform_361861	guanine nucleotide-binding protein subunit alpha-11	2.63	<0.01
			Thyroid hormone signaling pathway		
		isoform_113388	hypoxia-inducible factor 1 alpha	6.64	<0.01
		isoform_225372	mediator of RNA polymerase II transcription subunit 13	4.33	<0.01
			GnRH signaling pathway		
		isoform_326196	guanine nucleotide-binding protein	4.12	<0.01
Liver	3 MAH		Sphingolipid signaling pathway		
		isoform_209109	ceramide synthetase	3.75	<0.01
			Glycine, serine, and threonine metabolism		
		isoform_48613	alanine-glyoxylate transaminase	5.36	<0.01
		isoform_321441	5-aminolevulinate synthase	5.23	<0.01
		isoform_365726	L-pipecolate oxidase	4.51	<0.01
		isoform_41453	dihydrolipoamide dehydrogenase	3.62	<0.01
		isoform_257499	glycine amidinotransferase	3.56	<0.01
			Propanoate metabolism		
		isoform_296751	methylmalonyl-CoA mutase	7.18	<0.01
		isoform_41453	dihydrolipoamide dehydrogenase	3.62	<0.01
			Fat digestion and absorption		
		isoform_220933	aspartate aminotransferase	8.18	<0.01
		isoform_163445	fatty acid-binding protein	3.79	<0.01
		isoform_51344	apolipoprotein	3.76	<0.01
		isoform_317355	microsomal triglyceride transfer protein	3.64	<0.01
		isoform_293387	apolipoprotein	2.02	<0.01
			Glycerophospholipid metabolism		
		isoform_170346	glycerol-3-phosphate dehydrogenase (NAD+)	4.35	<0.01
		isoform_14990	ethanolamine-phosphate cytidyltransferase	3.43	<0.01
		isoform_245223	membrane dipeptidase	2.42	<0.01
		isoform_25396	glyceronephosphate O-acyltransferase	2.20	<0.01
		isoform_5689	phosphatidate phosphatase LPIN	2.08	<0.01
			Th17 cell differentiation		
		isoform_86026	molecular chaperone HtpG	9.36	<0.01
		isoform_125178	major histocompatibility complex, class II	5.40	<0.01
		isoform_354536	hypoxia-inducible factor 1 alpha	4.08	<0.01
			IL-17 signaling pathway		
		isoform_8916	transcription factor	3.58	<0.01
		isoform_32558	splicing factor, arginine/serine-rich 1	2.49	<0.01
			Fatty acid elongation		
		isoform_331832	long-chain 3-hydroxyacyl-CoA dehydrogenase	7.46	<0.01
		isoform_213152	very-long-chain (3R)-3-hydroxyacyl-CoA dehydratase	3.63	<0.01
Liver	9 MAH		Glycerolipid metabolism		
		isoform_129084	triose/dihydroxyacetone kinase	3.41	<0.01
		isoform_173628	glycerol kinase	3.36	<0.01
		isoform_294807	glycerol-3-phosphate O-acyltransferase 1/2	2.84	<0.01
			FoxO signaling pathway		
		isoform_27401	homer	3.78	<0.01
		isoform_361779	catalase	3.18	<0.01
		isoform_379101	5'-AMP-activated protein kinase	2.95	<0.01
		isoform_327226	B-Raf proto-oncogene serine/threonine-protein kinase	2.59	<0.01
		isoform_344831	forkhead box protein O3	2.28	<0.01
			PPAR signaling pathway		
		isoform_18527	carnitine O-palmitoyltransferase	8.63	<0.01
		isoform_220131	long-chain acyl-CoA synthetase	3.45	<0.01
		isoform_173628	glycerol kinase	3.36	<0.01
		isoform_33276	cholesterol 7 alpha-monooxygenase	3.26	<0.01
		isoform_20614	spermine oxidase	2.48	<0.01
			Glycine, serine, and threonine metabolism		
		isoform_37652	sarcosine oxidase/L-pipecolate oxidase	8.53	<0.01

Table 2. Cont.

Tissue	Period	Gene ID	Gene Description	Fold Change	p Value
		isoform_170963	guanidinoacetate N-methyltransferase	4.37	<0.01
		isoform_66322	2,3-bisphosphoglycerate-dependent phosphoglycerate mutase	3.63	<0.01
		isoform_323882	betaine-homocysteine S-methyltransferase	2.83	<0.01
			AMPK signaling pathway		
		isoform_66227	elongation factor 2	11.54	<0.01
		isoform_18527	carnitine O-palmitoyltransferase 1	8.63	<0.01
		isoform_117486	ribosomal protein S6 kinase beta	3.64	<0.01
		isoform_309342	hydroxymethylglutaryl-CoA reductase	3.44	<0.01
		isoform_379101	5'-AMP-activated protein kinase	2.95	<0.01
		isoform_344831	forkhead box protein O3	2.28	<0.01
			Insulin signaling pathway		
		isoform_12353	proto-oncogene C-crk	4.12	<0.01
		isoform_117486	ribosomal protein S6 kinase beta	3.64	<0.01
		isoform_240467	pyruvate kinase	3.28	<0.01
		isoform_313475	protein phosphatase 1 regulatory	3.12	<0.01
		isoform_379101	5'-AMP-activated protein kinase, regulatory gamma subunit	2.95	<0.01
		isoform_231208	glucokinase	2.72	<0.01
		isoform_327226	B-Raf proto-oncogene serine/threonine-protein kinase	2.59	<0.01
		isoform_3120	phosphorylase kinase	2.24	<0.01

Additionally, some genes involved in metabolism were identified. For example, the DEGs in the brain and liver encode energy-, nucleotide-, and glycolysis metabolism-related enzymes, cell signal transduction-related factors, and immune-response genes (Table 3). Furthermore, heat shock protein (HSP) and fatty acid binding protein (FABP) were expressed in both the brain and liver.

Table 3. Common differentially expressed genes in brain and liver tissues from fish with varying growth rates at two growth stages.

Period	Gene ID	Gene Description	Fold Change (Brain)	Fold Change (Liver)	p Value
3 MAH	Fatty acid elongation				
	isoform_119505	long-chain 3-hydroxyacyl-CoA dehydrogenase	−3.96	−5.23	<0.01
	isoform_213152	very-long-chain (3R)-3-hydroxyacyl-CoA dehydratase	2.80	3.63	<0.01
	isoform_331832	enoyl-CoA hydratase/long-chain 3-hydroxyacyl-CoA dehydrogenase	3.84	7.46	<0.01
	isoform_62084	acetyl-CoA acyltransferase	−5.76	−7.35	<0.01
	Th17 cell differentiation				
	isoform_62373	molecular chaperone HspG	−9.47	−9.10	<0.01
	isoform_148791	signal transducer and activator of transcription 3	−2.43	−1.61	<0.01
	isoform_42223	proto-oncogene protein c-fos	−2.15	−1.34	<0.01
	isoform_13757	interleukin 7 receptor	−1.86	−0.93	<0.01
	isoform_286564	immunoglobulin lambda-like polypeptide 1	−1.43	−3.33	<0.01
	isoform_110868	non-receptor tyrosine-protein kinase TYK2	−1.14	−0.38	<0.01
	isoform_132081	solute carrier family 30 (zinc transporter), member 10	1.35	0.00	<0.01
	isoform_354536	hypoxia-inducible factor 3 alpha	3.35	4.08	<0.01
	IL-17 signaling pathway				
	isoform_39669	major histocompatibility complex, class II	−3.44	−4.45	<0.01
	isoform_115641	molecular chaperone HspG	−2.79	−2.31	<0.01
	isoform_135192	prostaglandin-endoperoxide synthase 2	−2.49	−1.56	<0.01
	isoform_125178	major histocompatibility complex, class II	1.09	5.40	<0.01
	isoform_32558	splicing factor, arginine/serine-rich 1	2.14	2.49	<0.01
	isoform_354536	hypoxia-inducible factor 2 alpha	3.35	4.08	<0.01

Table 3. Cont.

Period	Gene ID	Gene Description	Fold Change (Brain)	Fold Change (Liver)	p Value
9 MAH	Insulin signaling pathway				
	isoform_158560	mitogen-activated protein kinase kinase 2	−5.76	−5.63	<0.01
	isoform_189742	mitogen-activated protein kinase kinase 2	−4.92	−5.64	<0.01
	isoform_189742	mitogen-activated protein kinase kinase 2	−4.92	−5.64	<0.01
	isoform_118529	atrophin-1 interacting protein 1	−3.84	−0.06	<0.01
	isoform_30052	mitogen-activated protein kinase kinase 1	−3.33	−1.72	<0.01
	isoform_27740	exocyst complex component 7	−1.74	−2.63	<0.01
	isoform_187116	hexokinase	−1.38	−0.43	<0.01
	isoform_107030	phosphoenolpyruvate carboxykinase	−1.30	−2.69	<0.01
	isoform_32627	MAP kinase interacting serine/threonine kinase	−1.19	−2.67	<0.01
	isoform_357827	RAF proto-oncogene serine/threonine-protein kinase	−1.17	−2.60	<0.01
	isoform_125524	SHC-transforming protein 2	−1.01	−2.76	<0.01
	isoform_66303	protein phosphatase 1 regulatory subunit 3A/B/C/D/E	−1.00	−3.68	<0.01
	isoform_117486	ribosomal protein S6 kinase beta	2.87	3.64	<0.01
	isoform_20826	Rap guanine nucleotide exchange factor 1	3.43	2.61	<0.01

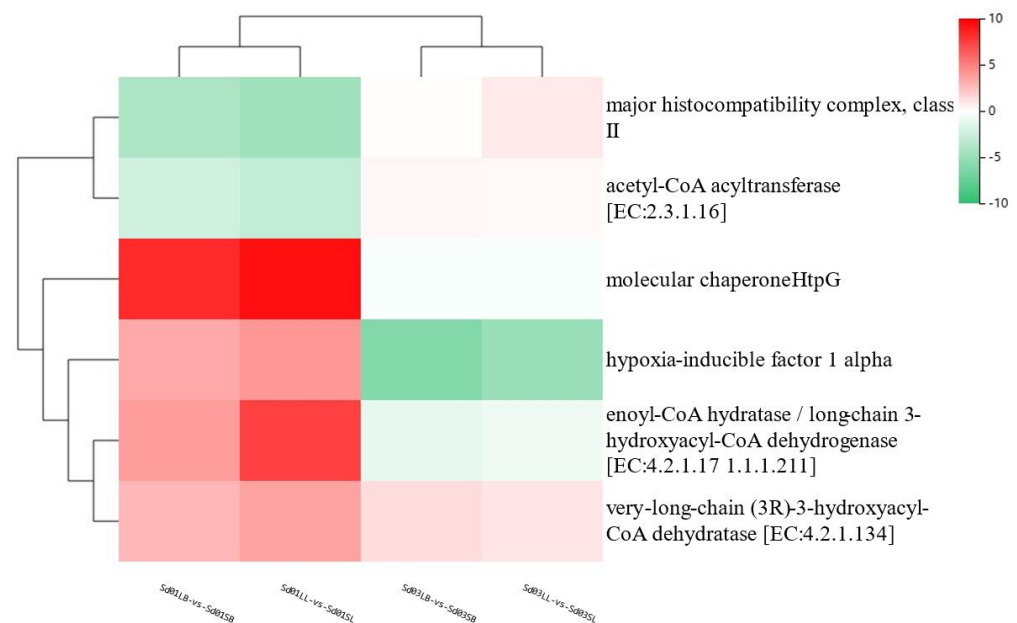


Figure 5. Heat-map analysis of selected common DEGs in brain and liver tissue of *S. d. denticulatus* in the FG and SG groups. FB, brain sample from the FG group; SB, brain sample from the SG group; FL, liver sample from the FG group; SL, liver sample from the SG group.

3.7. RT-qPCR Validation

RT-qPCR was employed to validate the RNA-seq results of six functional genes related to growth, specifically those involved in glycan biosynthesis (*SUL*), amino acid biosynthesis (*5-AS*), lipid metabolism (*ECH*), energy metabolism (*COD*), cellular communities (*VT*), and carbohydrate metabolism (*GK*). Primers for the above six genes were designed based on the sequences obtained from transcriptome sequencing. The collective data from the three stages are presented in Figure 6, including the data obtained from RNA-seq. The results indicated that the expression levels detected by RT-qPCR shared similar profiles with the data generated by RNA-seq, confirming that the RNA-seq data were reliable.

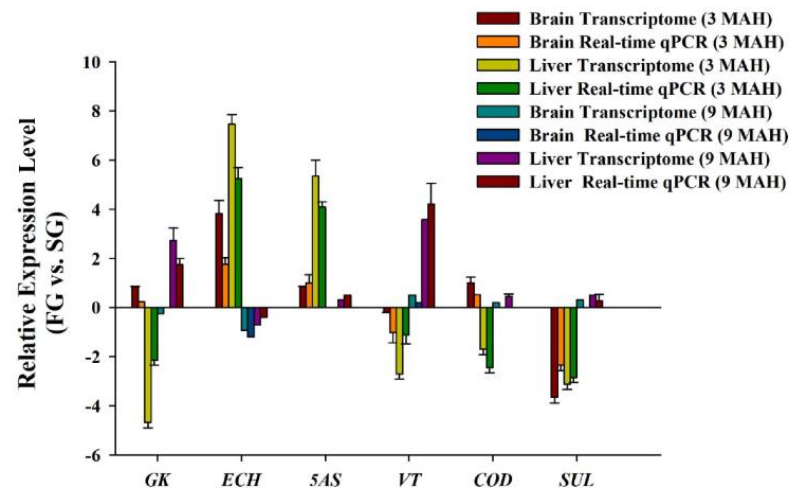


Figure 6. The transcriptome data from *S. d. denticulatus* were validated by RT-qPCR. The displayed values represent the ratio of gene expression levels between the fast-growing and slow-growing groups. Brain Transcriptome (3 MAH), the relative expression level in brain tissue at 3 months from transcriptome data; Brain Real-time qPCR (3 MAH), the relative expression level in brain tissue at 3 months from Real-time qPCR data; Liver Transcriptome (3 MAH), the relative expression level in liver tissue at 3 months from transcriptome data; Liver Real-time qPCR (3 MAH), the relative expression level in liver tissue at 3 months from Real-time qPCR data; Brain Transcriptome (9 MAH), the relative expression level in brain tissue at 9 months from transcriptome data; Brain Real-time qPCR (9 MAH), the relative expression level in brain tissue at 9 months from Real-time qPCR data; Liver Transcriptome (9 MAH), the relative expression level in liver tissue at 9 months from transcriptome data; Liver Real-time qPCR (9 MAH), the relative expression level in liver tissue at 9 months from Real-time qPCR data.

4. Discussion

S. d. denticulatus is a commercially valuable fish found in the Pearl River system in southern China. This species has several desirable traits, including good taste, large body size, and high environmental tolerance. However, the growth rate of *S. d. denticulatus* is slower than other carp species [37]. Growth speed is a crucial trait of farm fish, the faster growth rate will decrease the time it takes to grow a fish to market. Fish growth is a highly complex biological process involving cell proliferation, hormone biosynthesis, signal transduction, and interactions with the external environment [37]. To comprehensively understand the mechanisms underlying fish growth and development, identifying the biological pathways strongly associated with individual phenotypic traits is essential. Many studies show that hormones within the brain–liver axis primarily regulate metabolism, gonadal maturation, growth, and reproduction in fish. The endocrine system, which is predominantly influenced by exogenous signals, controls the nutritional status and growth of fish species. The brain is a key tissue that releases regulatory factors, including growth hormones (GHs), insulin-like growth factors (IGFs), growth hormone-releasing hormone (GHRH), and thyroid hormones [37,38]. In the brain, GH is secreted by the pituitary gland and stimulates growth by promoting protein synthesis and cell growth. The capacity of exogenous GH to enhance growth rates has been well documented in salmonids, allowing the prediction of growth-promoting effects based on the GH source and dose, rearing conditions, and fish strain. Somatostatin inhibits release of GH from the pituitary gland, thus maintaining a regulatory balance in the growth hormone axis [39]. GHRH, produced in the hypothalamus, normally stimulates the release of GH from the pituitary gland by inducing growth hormone mRNA expression in both embryonic and pituitary cells [40]. Thyroid hormones are essential for normal brain development and are crucial in the regulation of metabolism and growth. Thyroid hormones interact with the growth hormone axis, influencing growth rate and development [41]. In the liver,

GHRs are receptors for GH that are expressed in various tissues, including the liver, where they mediate the effects of GH by promoting IGF production. After GH binding, GHR undergoes conformational changes, activating the associated JAK2 kinases via the Janus kinase signal transducer and activator of transcription (JAK-STAT) pathway. These kinases phosphorylate specific tyrosine residues on the receptor, creating docking sites for the STAT protein. Phosphorylated STAT proteins dimerize and translocate to the nucleus, where they regulate the transcription of growth-related genes, including those encoding insulin-like growth factors (IGFs) [42]. Therefore, it is evident that the interaction of lipid elongation, the PI3K/Akt signaling pathway, and the GHRH signaling pathway in the brain and liver influences individual growth and development. Understanding the genes encoding these hormones and factors is critical for elucidating the mechanism of growth in fish, with the brain–liver axis being the central pathway in this process. Understanding these genetic mechanisms can aid in the selective breeding of fish to improve growth rates.

The RNA-seq results revealed that, in brain tissue, the PI3K/Akt and insulin signaling pathways, lipid metabolism, and protein metabolism were significantly upregulated at the early stage, whereas insulin secretion, GnRH, thyroid hormones, and the lipid metabolism pathway were significantly expressed at the later stage. In the liver, PI3K/Akt signaling, lipid biosynthesis, and amino acid metabolism were upregulated at 3 MAH, and glycerolipid biosynthesis, insulin signaling, and the FoxO signaling pathway were mainly upregulated at 9 MAH (Figure 3).

The PI3K/Akt pathway is a central signaling pathway that regulates various cellular processes, including growth, proliferation, survival, and metabolism. This pathway is activated by various extracellular signals, including growth factors, hormones, and cytokines [43]. The insulin signaling pathway is a critical regulator of glucose homeostasis and metabolism. Insulin, a hormone produced by the pancreas, has widespread effects on carbohydrate, fat, and protein metabolism [44,45]. These two pathways are regulated by hormones released from the brain that bind to the extracellular domain of GHR and induce receptor dimerization and activation. This activation leads to the phosphorylation of tyrosine residues in the intracellular domain of GHR by Janus kinase 2 (JAK2), which is associated with GHR. Additionally, phosphorylated GH provides docking sites for various signaling molecules, including insulin receptor substrates (IRSs) [46,47]. Moreover, IGF participates in the insulin signaling pathway to regulate metabolism, growth, and various cellular processes via insulin receptor activation, tyrosine kinase activation, IRS phosphorylation, and PI3K-Akt pathway activation [48,49]. Therefore, the genes encoding GHs were mainly upregulated in the early stages, whereas the genes for downstream regulation (insulin signaling) were highly expressed in the later stages of the brain. However, the liver, which is regulated by the brain, showed more DEGs in the PI3K/Akt signaling pathway, while more DEGs were identified in the insulin and FoxO signaling pathways. Heatmap analysis of genes from several pathways between the brain and liver tissues showed that the brain and liver showed similar trends in the expression of target genes, but these genes in the brain showed higher expression than those in the liver at an early stage. In contrast, at a later stage, DEGs from the liver showed higher expression than those from the brain (Figure 3). These results indicate that brain tissue first releases some GH and IGFs in the regulatory pathway, and then the regulatory factors interact with the liver and other tissues, triggering the corresponding pathways in the liver, especially the PI3K/Akt and insulin signaling pathways. And the thyroid hormones that were observed to have more DEGs at 9 MAH could interact with the GH axis. They regulate the production and secretion of GH from the anterior pituitary gland and influence the sensitivity of tissues to GH for regulating hormones at later stages.

Furthermore, the FoxO signaling pathway was identified in the brain tissue at 9 MAH. This pathway is closely associated with the synthesis and breakdown of muscle proteins [50]. In fish, the FoxO signaling pathway influences growth primarily through its involvement in nutrient sensing, cell proliferation, and apoptosis [51,52]. In particular, the FoxO pathway interacts with the IGF-1 signaling pathway, which is crucial for regulating fish growth.

Insulin and IGF-1 stimulate cell growth, proliferation, and survival through the activation of the sequential signaling pathways, including the PI3K/Akt pathway, and subsequent inhibition of FoxO transcriptional activity [53]. As growth regulators, DEGs encoding regulators of the FoxO signaling pathway were mainly observed at a later stage after GH regulation.

During the two growth stages, the pathways of amino acid metabolism and lipid metabolism were present in the FG groups. Leucine, isoleucine, and valine play roles in improving and regulating the metabolism of fats and sugars [26]. These three amino acids are among nine essential amino acids that share a common membrane transport system and function as enzymes for transamination and irreversible oxidation. Valine is metabolized into carbohydrates, whereas leucine and isoleucine are metabolized into ketogenic substances. Their end products, succinyl-CoA and/or acetyl-CoA, enter the Krebs cycle to produce energy and promote gluconeogenesis. Additionally, they can act as precursors of adipogenic and ketone bodies via acetyl-CoA and acetoacetate [54]. Moreover, fatty acids play a crucial role in maintaining normal bodily functions, promoting growth and development, and regulating immunity [55,56]. Fatty acids play pivotal roles in growth and development by serving as components of membrane lipids, acting as receptors and ligands for transcription factors that govern gene expression, functioning as precursors for eicosanoids, participating in cellular communication, and engaging in direct interactions with proteins [57]. Both pathways play key roles as building blocks of muscle growth and organ development in *S. d. denticulatus*.

5. Conclusions

In this study, the brain and liver transcriptomes of *S. d. denticulatus* at different growth rates at two growth stages were investigated. The transcriptome sequencing results suggest that the individual growth of *S. d. denticulatus* may be regulated by brain and liver interactions. Several key growth regulation pathways, including the PI3K/Akt and insulin signaling pathways, are first upregulated in the brain and later expressed in the liver. This study provides new insights into the growth regulation mechanisms of establishes a foundation for further research on the growth of *S. d. denticulatus* and enhances our understanding of the regulatory mechanisms governing individual fish growth.

Supplementary Materials: The following supporting information can be downloaded at: <https://www.mdpi.com/article/10.3390/fishes9100411/s1>, Table S1: Primers for qRT-PCR; Table S2: Overview of the RNA-Seq data.

Author Contributions: X.X. and J.Z. conducted the transcriptomic analysis and genotyping experiments of *S. d. denticulatus*. X.L., Z.X., W.L. (Wenlang Liang), Y.S. and L.L. participated in biological experiments and the final data analysis. W.L. (Weiqiang Lin) and J.X. were mainly responsible for project coordination. All authors reviewed and approved the final manuscript.

Funding: This study was supported by the National Natural Science Foundation of China (Approval No. 42106130), the Natural Science Foundation of Guangdong Province (Approval No. 2020A1515110237), and the Zhaoqing City Science and Technology Plan Project (Approval No. 2022N006).

Institutional Review Board Statement: This study was approved by the Institutional Animal Care and Use Committee and was conducted in accordance with the animal care and use guidelines of the Ethics Committee of Zhongkai College of Agriculture and Engineering. The approval number is 2020071109, and the approval date was 11 July 2020.

Data Availability Statement: Additional information and data for this study are available from the corresponding author and principal investigator.

Acknowledgments: The fish were provided by the Zhaoqing Fisheries Research Institute. The Zhaoqing Fisheries Research Institute provided breeding services and technical support for this study.

Conflicts of Interest: The authors declare no conflicts of interest.

References

- Lu, X.; Chen, H.M.; Qian, X.Q.; Gui, J.F. Transcriptome analysis of grass carp (*Ctenopharyngodon idella*) between fast- and slow-growing fish. *Comp. Biochem. Physiol. Part D Genom. Proteom.* **2020**, *35*, 100688. [\[CrossRef\]](#) [\[PubMed\]](#)
- De-Santis, C.; Jerry, D.R. Candidate growth genes in finfish—Where should we be looking? *Aquaculture* **2007**, *272*, 22–38. [\[CrossRef\]](#)
- Dai, X.; Zhang, W.; Zhuo, Z.; He, J.; Yin, Z. Neuroendocrine regulation of somatic growth in fishes. *Sci. China Life Sci.* **2015**, *58*, 137–147. [\[CrossRef\]](#) [\[PubMed\]](#)
- Boyce, W.T.; Sokolowski, M.B.; Robinson, G.E. Genes and environments, development and time. *Proc. Natl. Acad. Sci. USA* **2020**, *117*, 23235–23241. [\[CrossRef\]](#) [\[PubMed\]](#)
- Gjedrem, T.; Rye, M. Selection response in fish and shellfish: A review. *Rev. Aquac.* **2018**, *10*, 168–179. [\[CrossRef\]](#)
- Gjedrem, T.; Robinson, N.A. Advances by Selective Breeding for Aquatic Species: A Review. *Agric. Sci.* **2014**, *5*, 1152–1158. [\[CrossRef\]](#)
- Vieira Ventura, R.; Fonseca, E.S.F.; Manuel Yáñez, J.; Brito, L.F. Opportunities and challenges of phenomics applied to livestock and aquaculture breeding in South America. *Anim. Front.* **2020**, *10*, 45–52. [\[CrossRef\]](#)
- Houston, R.D.; Bean, T.P.; Macqueen, D.J.; Gundappa, M.K.; Jin, Y.H.; Jenkins, T.L.; Selly, S.L.C.; Martin, S.A.M.; Stevens, J.R.; Santos, E.M.; et al. Harnessing genomics to fast-track genetic improvement in aquaculture. *Nat. Rev. Genet.* **2020**, *21*, 389–409. [\[CrossRef\]](#)
- Johnston, I.A.; Bower, N.I.; Macqueen, D.J. Growth and the regulation of myotomal muscle mass in teleost fish. *J. Exp. Biol.* **2011**, *214 Pt 10*, 1617–1628. [\[CrossRef\]](#)
- Vélez, E.J.; Lutfi, E.; Azizi, S.; Perelló, M.; Salmerón, C.; Riera-Codina, M.; Ibarz, A.; Fernández-Borràs, J.; Blasco, J.; Capilla, E.; et al. Understanding fish muscle growth regulation to optimize aquaculture production. *Aquaculture* **2017**, *467*, 28–40. [\[CrossRef\]](#)
- Su, J.; Li, W.; Li, H.; Zhou, Z.; Miao, Y.; Yuan, Y.; Li, Y.; Tao, M.; Zhang, C.; Zhou, Y.; et al. Comparative transcriptomic analysis of the brain-liver Axis reveals molecular mechanisms underlying acute cold stress response in Gynogenetic Mrigal carp. *Aquaculture* **2024**, *588*, 740908. [\[CrossRef\]](#)
- Zhou, L.; Yang, R.; Tian, H.; Qin, X.; Ye, C.; Shi, X.; Xia, C.; Cai, T.; Xie, Y.; Jia, Y.; et al. Sexual dimorphism in *Odontobutis sinensis* brain-pituitary-gonad axis and liver highlighted by histological and transcriptomic approach. *Gene* **2022**, *819*, 146264. [\[CrossRef\]](#) [\[PubMed\]](#)
- Luo, W.; Chi, S.; Wang, J.; Yu, X.; Tong, J. Comparative transcriptomic analyses of brain-liver-muscle in channel catfish (*Ictalurus punctatus*) with differential growth rate. *Comp. Biochem. Physiol. Part D Genom. Proteom.* **2024**, *49*, 101178. [\[CrossRef\]](#) [\[PubMed\]](#)
- Degani, G. Somatolactin Transcription during Oogenesis in Female Blue Gourami (*Trichogaster trichopterus*). *Adv. Biol. Chem.* **2015**, *5*, 279–285. [\[CrossRef\]](#)
- Degani, G. Oogenesis control in multi-spawning blue gourami (*Trichogaster trichopterus*) as a model for the Anabantidae family. *Science* **2016**, *5*, 179–184.
- Degani, G.; Schreibman, M. Pheromone of male blue gourami and its effect on vitellogenesis, steroidogenesis and gonadotropin cells in pituitary of the female. *J. Fish Biol.* **2005**, *43*, 475–485. [\[CrossRef\]](#)
- Degani, G. Effect of sexual behavior on oocyte development and steroid changes in *Trichogaster trichopterus* (Pallas). *Copeia* **1993**, *1993*, 1091–1096. [\[CrossRef\]](#)
- Matsubara, Y.; Kiyohara, H.; Teratani, T.; Mikami, Y.; Kanai, T. Organ and brain crosstalk: The liver-brain axis in gastrointestinal, liver, and pancreatic diseases. *Neuropharmacology* **2022**, *205*, 108915. [\[CrossRef\]](#)
- Fu, B.; Wang, X.; Feng, X.; Yu, X.; Tong, J. Comparative transcriptomic analyses of two bighead carp (*Hypophthalmichthys nobilis*) groups with different growth rates. *Comp. Biochem. Physiol. Part D Genom. Proteom.* **2016**, *20*, 111–117. [\[CrossRef\]](#)
- Fu, B.; Yu, X.; Tong, J.; Pang, M.; Zhou, Y.; Liu, Q.; Tao, W. Comparative transcriptomic analysis of hypothalamus-pituitary-liver axis in bighead carp (*Hypophthalmichthys nobilis*) with differential growth rate. *BMC Genom.* **2019**, *20*, 328. [\[CrossRef\]](#)
- Mun, S.H.; You, J.H.; Oh, H.J.; Lee, C.H.; Baek, H.J.; Lee, Y.D.; Kwon, J.Y. Expression Patterns of Growth Related Genes in Juvenile Red Spotted Grouper (*Epinephelus akaara*) with Different Growth Performance after Size Grading. *Dev. Reprod.* **2019**, *23*, 35–42. [\[CrossRef\]](#) [\[PubMed\]](#)
- Reinecke, M.; Schmid, A.; Ermatinger, R.; Löffing-Cueni, D. Insulin-like growth factor I in the teleost *Oreochromis mossambicus*, the tilapia: Gene sequence, tissue expression, and cellular localization. *Endocrinology* **1997**, *138*, 3613–3619. [\[CrossRef\]](#) [\[PubMed\]](#)
- Otteson, D.C.; Cirenza, P.F.; Hitchcock, P.F. Persistent neurogenesis in the teleost retina: Evidence for regulation by the growth-hormone/insulin-like growth factor-I axis. *Mech. Dev.* **2002**, *117*, 137–149. [\[CrossRef\]](#) [\[PubMed\]](#)
- Kumar, V.; Khalil, W.K.B.; Weiler, U.; Becker, K. Influences of incorporating detoxified *Jatropha curcas* kernel meal in common carp (*Cyprinus carpio* L.) diet on the expression of growth hormone- and insulin-like growth factor-1-encoding genes. *J. Anim. Physiol. Anim. Nutr.* **2013**, *97*, 97–108. [\[CrossRef\]](#) [\[PubMed\]](#)
- Lin, G.; Thevasagayam, N.M.; Wan, Z.Y.; Ye, B.Q.; Yue, G.H. Transcriptome Analysis Identified Genes for Growth and Omega-3/-6 Ratio in Saline Tilapia. *Front. Genet.* **2019**, *10*, 244. [\[CrossRef\]](#)
- Kim, W.K.; Singh, A.K.; Wang, J.; Applegate, T. Functional role of branched chain amino acids in poultry: A review. *Poult. Sci.* **2022**, *101*, 101715. [\[CrossRef\]](#)

27. Vázquez, M.J.; Novelle, M.G.; Rodríguez-Pacheco, F.; Lage, R.; Varela, L.; López, M.; Pinilla, L.; Tena-Sempere, M.; Diéguez, C. AMPK-Dependent Mechanisms but Not Hypothalamic Lipid Signaling Mediates GH-Secretory Responses to GHRH and Ghrelin. *Cells* **2020**, *9*, 1940. [\[CrossRef\]](#)
28. Yin, M.; Zhang, L. Hippo signaling: A hub of growth control, tumor suppression and pluripotency maintenance. *J. Genet. Genom.* **2011**, *38*, 471–481. [\[CrossRef\]](#)
29. Ndandala, C.B.; Zhou, Q.; Li, Z.; Guo, Y.; Li, G.; Chen, H. Identification of Insulin-like Growth Factor (IGF) Family Genes in the Golden Pompano, *Trachinotus ovatus*: Molecular Cloning, Characterization and Gene Expression. *Int. J. Mol. Sci.* **2024**, *25*, 2499. [\[CrossRef\]](#)
30. Sun, P.; Yin, F.; Tang, B. Effects of Acute Handling Stress on Expression of Growth-Related Genes in *Pampus argenteus*: Gene expression during stress in pampus. *J. World Aquac. Soc.* **2017**, *48*, 166–179. [\[CrossRef\]](#)
31. Pang, X.; Cao, Z.D.; Fu, S.J. The effects of temperature on metabolic interaction between digestion and locomotion in juveniles of three cyprinid fish (*Carassius auratus*, *Cyprinus carpio* and *Spinibarbus sinensis*). *Comp. Biochem. Physiol. A Mol. Integr. Physiol.* **2011**, *159*, 253–260. [\[CrossRef\]](#) [\[PubMed\]](#)
32. Duan, B.; Chen, Q.; Liu, P.; Chi, C.; Yang, H. Studies on Status of Fishery Resources in Three Gorges Reservoir Reaches of the Yangtze River. *Acta Hydrobiol. Sin.* **2002**, *26*, 605–611.
33. Iversen, M.; Finstad, B.; McKinley, R.S.; Eliassen, R.A. The efficacy of metomidate, clove oil, Aqui-S™ and Benzoak® as anaesthetics in Atlantic salmon (*Salmo salar* L.) smolts, and their potential stress-reducing capacity. *Aquaculture* **2003**, *221*, 549–566. [\[CrossRef\]](#)
34. Langmead, B.; Salzberg, S.L. Fast gapped-read alignment with Bowtie 2. *Nat. Methods* **2012**, *9*, 357–359. [\[CrossRef\]](#) [\[PubMed\]](#)
35. Acharya, U.R.; Behera, S.; Swain, S.; Panda, M.K.; Mistri, A.R.; Sahoo, B. Sequence and structural analysis of β -actin protein of fishes, using bioinformatics tools and techniques. *Int. J. Biosci.* **2014**, *4*, 249–256.
36. Liu, Z.J.; Zhu, Z.Y.; Roberg, K.; Faras, A.; Guise, K.; Kapuscinski, A.R.; Hackett, P.B. Isolation and characterization of beta-actin gene of carp (*Cyprinus carpio*). *DNA Seq.* **1990**, *1*, 125–136. [\[CrossRef\]](#)
37. Dutta, H. Growth in fishes. *Gerontology* **1994**, *40*, 97–112. [\[CrossRef\]](#)
38. Pogoda, H.M.; Hammerschmidt, M. Molecular genetics of pituitary development in zebrafish. *Semin. Cell Dev. Biol.* **2007**, *18*, 543–558. [\[CrossRef\]](#)
39. Sheridan, M.A.; Hagemeister, A.L. Somatostatin and somatostatin receptors in fish growth. *Gen. Comp. Endocrinol.* **2010**, *167*, 360–365. [\[CrossRef\]](#)
40. Nam, B.H.; Moon, J.Y.; Kim, Y.O.; Kong, H.J.; Kim, W.J.; Kim, K.K.; Lee, S.J. Molecular and functional analyses of growth hormone-releasing hormone (GHRH) from olive flounder (*Paralichthys olivaceus*). *Comp. Biochem. Physiol. B Biochem. Mol. Biol.* **2011**, *159*, 84–91. [\[CrossRef\]](#)
41. Bernal, J. Thyroid Hormones in Brain Development and Function. In *Endotext*; Feingold, K.R., Anawalt, B., Blackman, M.R., Boyce, A., Chrousos, G., Corpas, E., de Herder, W.W., Dhatariya, K., Dungan, K., Hofland, J., et al., Eds.; MDText.com, Inc.: South Dartmouth, MA, USA, 2000.
42. Carter-Su, C.; Schwartz, J.; Argetsinger, L.S. Growth hormone signaling pathways. *Growth Horm. IGF Res.* **2016**, *28*, 11–15. [\[CrossRef\]](#) [\[PubMed\]](#)
43. Yu, J.S.; Cui, W. Proliferation, survival and metabolism: The role of PI3K/AKT/mTOR signalling in pluripotency and cell fate determination. *Development* **2016**, *143*, 3050–3060. [\[CrossRef\]](#) [\[PubMed\]](#)
44. Li, C.; Zhang, B.B. Insulin signaling and action: Glucose, lipids, protein. In *Endotext*; Feingold, K.R., Anawalt, B., Blackman, M.R., Boyce, A., Chrousos, G., Corpas, E., de Herder, W.W., Dhatariya, K., Dungan, K., Hofland, J., et al., Eds.; MDText.com, Inc.: South Dartmouth, MA, USA, 2000.
45. Norton, L.; Shannon, C.; Gastaldelli, A.; DeFronzo, R.A. Insulin: The master regulator of glucose metabolism. *Metabolism* **2022**, *129*, 155142. [\[CrossRef\]](#) [\[PubMed\]](#)
46. Zhang, Y.; Jiang, J.; Kopchick, J.J.; Frank, S.J. Disulfide linkage of growth hormone (GH) receptors (GHR) reflects GH-induced GHR dimerization. Association of JAK2 with the GHR is enhanced by receptor dimerization. *J. Biol. Chem.* **1999**, *274*, 33072–33084. [\[CrossRef\]](#) [\[PubMed\]](#)
47. Campbell, G.S. Growth-hormone signal transduction. *J. Pediatr.* **1997**, *131 Pt 2*, S42–S44. [\[CrossRef\]](#) [\[PubMed\]](#)
48. Hakuno, F.; Takahashi, S.I. IGF1 receptor signaling pathways. *J. Mol. Endocrinol.* **2018**, *61*, T69–T86. [\[CrossRef\]](#) [\[PubMed\]](#)
49. Werner, H. The IGF1 Signaling Pathway: From Basic Concepts to Therapeutic Opportunities. *Int. J. Mol. Sci.* **2023**, *24*, 14882. [\[CrossRef\]](#)
50. Zhang, L.; Li, X.; Yu, Y.; Zhang, L.; Dong, L.; Gan, J.; Mao, T.; Liu, T.; Peng, J.; He, L. Comparative analyses of liver transcriptomes reveal the effect of exercise on growth-, glucose metabolism-, and oxygen transport-related genes and signaling pathways in grass carp (*Ctenopharyngodon idella*). *Comp. Biochem. Physiol. A Mol. Integr. Physiol.* **2021**, *262*, 111081. [\[CrossRef\]](#)
51. Boccitto, M.; Kalb, R.G. Regulation of Foxo-dependent transcription by post-translational modifications. *Curr. Drug Targets* **2011**, *12*, 1303–1310. [\[CrossRef\]](#)
52. Zhang, T.; Zhang, M.; Sun, Y.; Li, L.; Cheng, P.; Li, X.; Wang, N.; Chen, S.; Xu, W. Identification and Functional Analysis of foxo Genes in Chinese Tongue Sole (*Cynoglossus semilaevis*). *Int. J. Mol. Sci.* **2023**, *24*, 7625. [\[CrossRef\]](#)

53. Luo, W.; Zhou, Y.; Wang, J.; Yu, X.; Tong, J. Identifying Candidate Genes Involved in the Regulation of Early Growth Using Full-Length Transcriptome and RNA-Seq Analyses of Frontal and Parietal Bones and Vertebral Bones in Bighead Carp (*Hypophthalmichthys nobilis*). *Front. Genet.* **2020**, *11*, 603454. [[CrossRef](#)] [[PubMed](#)]
54. Adeva-Andany, M.M.; López-Maside, L.; Donapetry-García, C.; Fernández-Fernández, C.; Sixto-Leal, C. Enzymes involved in branched-chain amino acid metabolism in humans. *Amino Acids* **2017**, *49*, 1005–1028. [[CrossRef](#)] [[PubMed](#)]
55. Calder, P.C. Functional Roles of Fatty Acids and Their Effects on Human Health. *JPEN J. Parenter. Enter. Nutr.* **2015**, *39* (Suppl. S1), 18s–32s. [[CrossRef](#)] [[PubMed](#)]
56. Innis, S.M. Fatty acids and early human development. *Early Hum. Dev.* **2007**, *83*, 761–766. [[CrossRef](#)]
57. de Carvalho, C.; Caramujo, M.J. The Various Roles of Fatty Acids. *Molecules* **2018**, *23*, 2583. [[CrossRef](#)]

Disclaimer/Publisher’s Note: The statements, opinions and data contained in all publications are solely those of the individual author(s) and contributor(s) and not of MDPI and/or the editor(s). MDPI and/or the editor(s) disclaim responsibility for any injury to people or property resulting from any ideas, methods, instructions or products referred to in the content.